Title
A neuronal signature for monogamous reunion

Journal
Proceedings of the National Academy of Sciences of the United States of America, 117(20)

ISSN
0027-8424

Authors
Scribner, Jennifer L
Vance, Eric A
Protter, David SW
et al.

Publication Date
2020-05-19

DOI
10.1073/pnas.1917287117

Peer reviewed

A neuronal signature for monogamous reunion

Jennifer L. Scribner[a], Eric A. Vance[b], David S. W. Protter[c], William M. Sheeran[d], Elliott Saslow[e], Ryan T. Cameron[e], Eric M. Klein[f], Jessica C. Jimenez[g], Mazen A. Kheirbek[h], and Zoe R. Donaldson[c,i,1]

[a]Department of Neuroscience, Mortimer B. Zuckerman Mind Brain Behavior Institute, Columbia University, New York, NY 10027; [b]Department of Applied Mathematics, University of Colorado Boulder, Boulder, CO 80309; [c]Department of Molecular, Cellular, and Developmental Biology, University of Colorado Boulder, Boulder, CO 80309; [d]Medical Scientist Training Program, University of Colorado Anschutz Medical School, Aurora, CO 80045; [e]College of Engineering & Applied Science, University of Colorado Boulder, Boulder, CO 80309; [f]Neuroscience Graduate Program, Brown University, Providence, RI 02912; [g]Medical Scientist Training Program, Columbia University, New York, NY 10032; [h]Department of Psychiatry, University of California, San Francisco, CA 94158; and [i]Department of Psychology and Neuroscience, University of Colorado Boulder, Boulder, CO 80309

Edited by Gene E. Robinson, University of Illinois at Urbana–Champaign, Urbana, IL, and approved March 28, 2020 (received for review October 3, 2019)

Pair-bond formation depends vitally on neuromodulatory signaling within the nucleus accumbens, but the neuronal dynamics underlying this behavior remain unclear. Using 1-photon in vivo Ca^{2+} imaging in monogamous prairie voles, we found that pair bonding does not elicit differences in overall nucleus accumbens Ca^{2+} activity. Instead, we identified distinct ensembles of neurons in this region that are recruited during approach to either a partner or a novel vole. The partner-approach neuronal ensemble increased in size following bond formation, and differences in the size of approach ensembles for partner and novel voles predict bond strength. In contrast, neurons comprising departure ensembles do not change over time and are not correlated with bond strength, indicating that ensemble plasticity is specific to partner approach. Furthermore, the neurons comprising partner and novel-approach ensembles are nonoverlapping while departure ensembles are more overlapping than chance, which may reflect another key feature of approach ensembles. We posit that the features of the partner-approach ensemble and its expansion upon bond formation potentially make it a key neuronal substrate associated with bond formation and maturation.

prairie vole | nucleus accumbens | pair bond | ensemble | calcium imaging

In fewer than 10% of mammalian species, humans included, individuals form mating-based pair bonds (1, 2). Pair bonds are maintained and reinforced over time by a selective desire to seek ptout and interact with a bonded partner. This behavior is not exhibited by most laboratory rodents, including mice and rats. However, in monogamous prairie voles, pair bonding is easily assessed using a test in which the focal animal chooses between spending time with a pair-bonded partner or a novel opposite-sex vole tethered on opposite sides of a testing chamber (3, 4). This partner-preference test provides an opportunity to examine neural activity while an animal is displaying a pair bond and to assess how behavior and neural activity change as a bond matures.

The nucleus accumbens (NAc) plays a large role in reward and motivation (5), making it a likely brain region for encoding highly rewarding pair bonds (6). When participants in a functional MRI study thought that they were holding hands with their pair-bonded partner, rather than an unfamiliar individual, they exhibited an enhanced blood oxygenation signal in the NAc (7). In prairie voles, disruption of neuromodulatory signaling within this region impairs bond formation (6), and subsequent gene expression changes contribute to bond maintenance (8, 9). In addition, activation of prefrontal projections to the NAc is sufficient to induce bond formation in the absence of mating (10). However, despite substantial evidence that the NAc plays a primary role in encoding pair bonds, the neuronal dynamics underlying this process and how they change as a bond progresses remain unexplored. Thus, we performed in vivo Ca^{2+} imaging in the NAc of freely behaving prairie voles before and after they mated to gain insight into how pair-bond formation and maturation are represented in the brain.

Results

Optimization of In Vivo Ca^{2+} Imaging in Prairie Voles. In vivo Ca^{2+} imaging is tractable in prairie voles. We used 1-photon microendoscopes, in combination with virally delivered synapsin-driven GCaMP6f (11), a fluorescent Ca^{2+} indicator (Fig. 1 *A*–*E*; lens placements in *SI Appendix*, Fig. S1), to image putative NAc neuronal activity in freely moving prairie voles. Our final dataset consisted of 17 voles (7 males, 10 females). We implanted lenses in 30 voles, 26 of which had observable fluorescence 4 wk post surgery. Of these, animals were excluded for the following reasons: lens placement outside of NAc ($n = 1$), <5 detectable putative cells ($n = 1$), lack of detectable partner preference during either partner preference test ($n = 3$; see below), and occluded field of view/motion artifact/technical problems ($n = 4$).

On average, we identified 43 ± 20 cells per animal per imaging session (range: 5 to 117). A repeated measures ANOVA showed that the average number of cells did not change across three imaging sessions spanning 20 d ($F_{(2, 38)} = 0.034$, $P = 0.967$). We took the average $\Delta F/F_0$ for each cell for the first 60 s and the last 60 s of the imaging sessions. During these epochs, the animal was housed alone with no access to stimuli, serving as a measure of baseline activity. There was no significant difference in the

Significance

Monogamous prairie voles form lifelong pair bonds, but the neuronal dynamics that underlie bond formation and maintenance in this species remain largely unknown. We performed imaging of populations of neurons while voles interacted with their pair-bonded partner or a novel vole before and after bond formation. We identified neurons that were active during partner approach and found that this subset of cells was distinct from those that were active during novel approach. Furthermore, the number of partner approach cells increased following bond formation, reflecting the emergence of bonding behaviors and correlating with bond strength. This discovery sheds light on how pair bonds may be encoded within the brain and what changes as bonds mature.

Author contributions: Z.R.D. designed research; J.L.S., E.M.K., and Z.R.D. performed research; J.C.J. and M.A.K. contributed new reagents/analytic tools; J.C.J. and M.A.K. provided training in calcium imaging and feedback/discussion of results; E.A.V., D.S.W.P., W.M.S., E.S., R.T.C., and Z.R.D. analyzed data; and Z.R.D. wrote the paper.

The authors declare no competing interest.

This article is a PNAS Direct Submission.

Data deposition: MATLAB scripts are available from the GitHub repository at https://github.com/donaldsonlab/monogamousreunion. Additional data supporting the findings of this study are available on Figshare at https://doi.org/10.6084/m9.figshare.8330102, https://doi.org/10.6084/m9.figshare.8330111, and https://doi.org/10.6084/m9.figshare.8330150.

See online for related content such as Commentaries.

[1]To whom correspondence may be addressed. Email: zoe.donaldson@colorado.edu.

This article contains supporting information online at https://www.pnas.org/lookup/suppl/doi:10.1073/pnas.1917287117/-/DCSupplemental.

First published May 7, 2020.

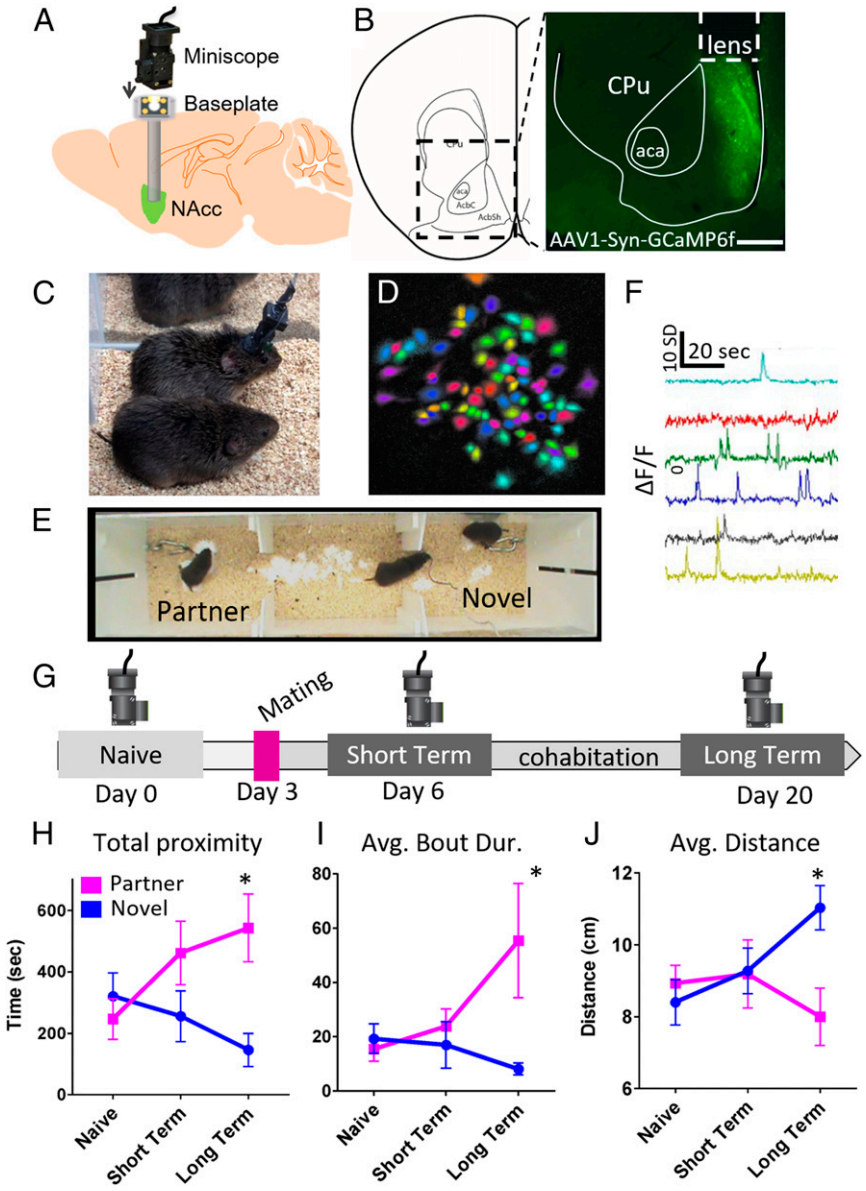

Fig. 1. Ca^{2+} imaging in monogamous prairie voles. (*A*) Voles were injected with AAV1-hSyn-GCaMP6f, and a GRIN lens was implanted into the NAc. After recovery, a baseplate was permanently affixed to the skull to enable placement of the miniscope. (*B*) Expression of GCaMP6f and lens insertion site. (Scale bar: 500 μm.) (*C*) Two voles huddling during an imaging session. (*D*) Putative neurons identified within the field of view of one animal. (*E*) Imaging sessions were carried out during a 20-min partner preference test. The test animal (center) with scope attached could freely move between two opposite sex animals tethered at either end of the apparatus. (*F*) The dF/F traces for six putative neurons. (*G*) Experimental time course showing imaging sessions undertaken in sexually naive individuals (day 0) and at short-term (day 6) and long-term (day 20) time points after partner introduction and mating. Animals cohabited with their partner continuously beginning on day 3. (*H–J*) Differences in social choice behavior emerged during the long-term imaging session. Test animals spent more time in proximity (<10 cm) (*H*), exhibited longer interaction bouts (*I*), and were physically closer to their mating partner (*J*) during the long-term imaging time point but did not exhibit differences in these metrics at the naive or short-term imaging sessions. All error bars are SE. *H*, $*P = 0.009$; *I*, $*P = 0.014$; *J*, $*P = 0.006$. See lens placements in *SI Appendix*, Fig. S1 and additional behavioral analysis in *SI Appendix*, Fig. S2. Data are available at https://doi.org/10.6084/m9.figshare.8330102.

average $\Delta F/F_0$ between the baselines at any of the imaging time points (naive: $T_{(614)} = 1.583$, $P = 0.114$, d = 0.0638; short term: $T_{(595)} = -0.353$, $P = 0.724$, d = −0.0145; long term: $T_{(639)} = 1.802$, $P = 0.072$, d = 0.0712). We combined these two epochs to generate a single baseline measure of $\Delta F/F_0$ per animal per time point.

Partner Preference Is Evident during Imaging Sessions. Prairie vole pair bonds are hallmarked by a selective preference to interact with a monogamous partner in a partner preference test. We imaged prairie voles in a 20-min partner preference test at three time points spanning pair-bond formation: when test animals were sexually naive (day 0), at a short-term time point following mating and cohabitation (day 6), and again at a long-term time point following mating and cohabitation (day 20) (Fig. 1*G*). As expected, sexually naive animals did not exhibit a preference prior to mating, and we observed the emergence and strengthening of partner preference following mating and cohabitation (12). Specifically, we found that test voles spent more time near their partner than the stranger (percentage of partner interaction relative to total interaction) by the long-term time point (Fig. 1 and *SI Appendix*, Fig. S2*D*; one-way *t* test relative to null value of

50%—naive: $t_{16} = -0.902$, $P = 0.381$, d = −0.219; short term: $t_{16} = 0.928$, $P = 0.367$, d = 0.225; long term: $t_{16} = 2.958$, $P = 0.009$, d = 0.717). Accordingly, the amount of time spent with the partner or novel animal was highly correlated with chamber time (*SI Appendix*, Table S1). Test animals also exhibited longer periods of interaction (interaction bouts) with their partner than with the stranger following mating (Figs. 1*I* and 2*A* and *SI Appendix*, Fig. S2*C*) (repeated measures ANOVA—time point: $F_{(2, 26)} = 0.419$, $P = 0.662$, $\eta^2 = 0.031$; tethered vole: $F_{(1, 13)} = 6.358$, $P = 0.026$, $\eta^2 = 0.328$; time point × tethered vole: $F_{(2, 26)} = 2.633$, $P = 0.091$. $\eta^2 = 0.168$; paired *t* test–naive: $t_{16} = 0.617$, $P = 0.546$, d = 0.150; short term: $t_{14} = -2.247$, $P = 0.041$, d = −0.580; long term: $t_{15} = -2.766$, $P = 0.014$, d = 0.692). Finally, we also examined the average distance between the test animal and tethered animal when the test animal was in the partner or novel chamber. We found that after mating and cohabitation, the test animal was closer to its partner than to the novel animal when it was in the respective chamber (Fig. 1*J*) (repeated measures ANOVA—time point: $F_{(2, 26)} = 0.172$, $P = 0.843$, $\eta^2 = 0.012$, chamber: $F_{(1, 13)} = 5.163$, $P = 0.039$, $\eta^2 = 0.269$, time point × chamber: $F_{(2, 26)} = 2.959$, $P = 0.068$, $\eta^2 = 0.174$; paired *t* test–naive: $t_{16} = 0.617$, $P = 0.414$, d = 0.204; short term: $t_{14} = -0.805$, $P = 0.434$, d = −0.208; long term: $t_{16} = -3.156$, $P = 0.006$, d = −0.765). Thus, overall interaction time, average social bout duration, and distance from stimulus animal while in the chamber all reflect the formation of a partner preference. These data also indicate that longer cohabitation leads to stronger bonds, enabling us to ask whether bond strength is represented in patterns of NAc neuron activity.

We were concerned that the brevity of the imaging sessions and attachment of the scope might impact our ability to detect partner preference. Therefore, we also performed a traditional 3-h partner preference test following each of the short- and long-term imaging sessions (days 7 and 21). We observed partner preference during the 3-h test at both time points (*SI Appendix*, Fig. S2*E*) (one-way *t* test relative to null value of 50%—short term: $t_{19} = 2.175$, $P = 0.043$, d = 0.486; long term: $t_{19} = 2.536$, $P = 0.020$, d = 0.567). The percentage of time interacting with

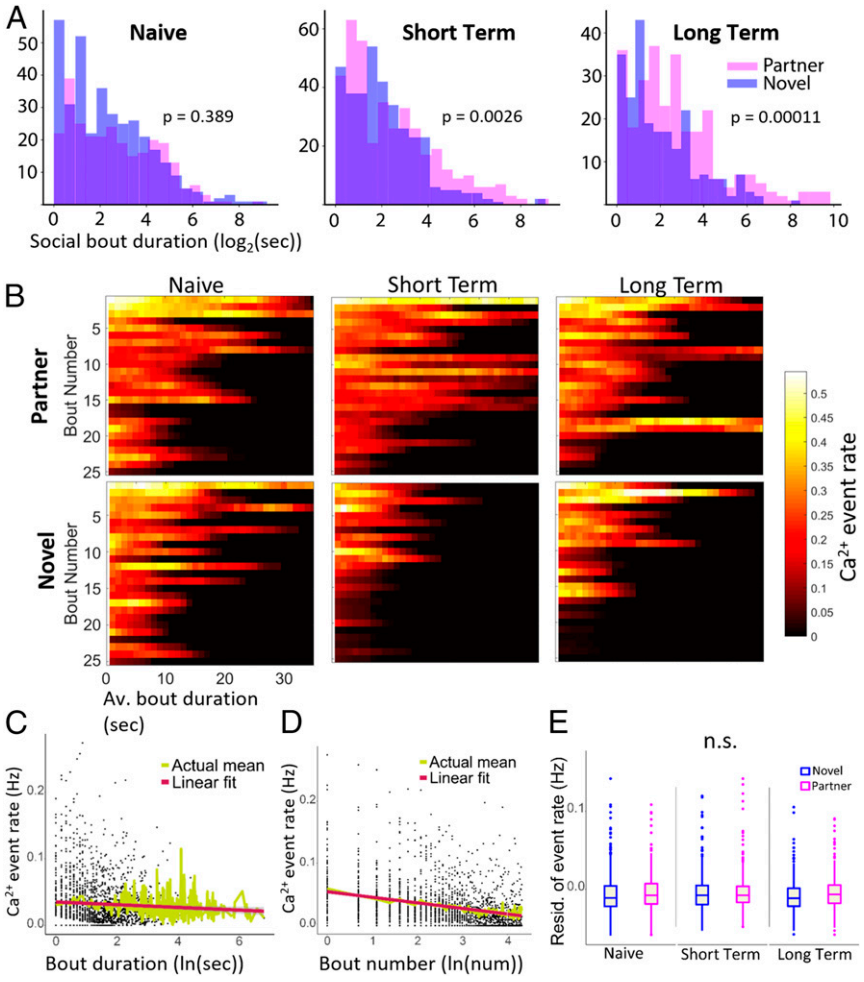

Fig. 2. Intensity of Ca^{2+} activity across interaction bouts with different tethered animals pre and post bonding. (*A*) Histograms showing frequency of social interaction bout lengths with partner (pink) and with novel (blue) animals. After mating/cohabitation, test animals had longer interaction bouts with their partner than with the novel individual. (*B*) Heat plots show the average Ca^{2+} transient events (Hz) pooled across all cells and animals. Rows for social interaction bouts represent the average across all animals and were truncated at 35 s and 25 bouts or when data were available for fewer than three animals. Bout length decreased across the test session and did not differ between stimulus animals during the sexually naive imaging session. In contrast, test animals exhibited longer and more interaction bouts with their mating partner than the novel individual during the short- and long-term imaging sessions. (*C*) Ca^{2+} activity was greater in short bouts than long bouts and corresponded with a logarithmic decrease in activity as bout length increased. (*D*) Activity was greater during initial interaction bouts within a session and exhibited a logarithmic decrease across subsequent social interaction bouts. (*E*) After controlling for differences in bout number and bout length, there were no significant differences in average calcium activity during partner and novel interaction. Residuals are plotted after regressing firing rate~ln(duration)+ln(bout number). Individual data are plotted in *SI Appendix*, Fig. S3. Data are available at https://doi.org/10.6084/m9.figshare.8330111.

the partner was correlated across the two time points (Spearman nonparametric test: $\rho = 0.537$, $P = 0.015$), while this was not observed across tests conducted during imaging sessions (Spearman nonparametric test: $\rho = -0.083$, $P = 0.751$). Three test animals showed a consistent preference for the novel animal in both 3-h tests, so we excluded these animals from subsequent analyses. Unlike the 20-min test, partner preference was evident even at the short-term time point in the 3-h test (*SI Appendix*, Fig. S2 *D* and *E*), and partner interaction was correlated across the time points. This suggests that the traditional 3-h partner preference test is more sensitive and consistent than the 20-min version employed during imaging sessions; however, viewed together, these data serve to confirm the emergence and strengthening of a partner preference following mating and cohabitation.

Population Activity Does Not Differ between Partner and Novel Interaction. Based on human neuroimaging studies (7), we hypothesized that overall neuronal activity in the NAc would be greater when a pair-bonded vole interacted with its partner relative to when it was with a stranger. Unexpectedly, activity across all putative NAc neurons, reported as the event rates of imaged Ca^{2+} transients, did not predict whether the test animal was interacting with its partner or with the novel individual after controlling for differences in the duration of a test vole's interactions with each tethered animal. We defined all periods of social interaction during the partner preference test that were at least 1 s in duration as social bouts. In sexually naive animals, social bout duration did not differ across the interactions with two novel voles; however, following mating, test animals had longer social bouts with their partner than with a novel tethered animal (Fig. 2*A*) (permutation analysis on bout duration—naive: $P = 0.389$; short term: $P = 0.00255$; long term: $P = 0.00011$). As with other metrics of partner preference (Fig. 1 *H*–*J*), the difference in partner and novel social bout duration became more significant with longer cohabitation and mating (Fig. 2*A*).

We found that the average population activity rate was greater during initial social bouts and at the beginning of a bout (linear regression, $P < 0.0001$ for both factors) (Fig. 2 *B*–*D* and *SI Appendix*, Fig. S3). As voles display differences in social behavior

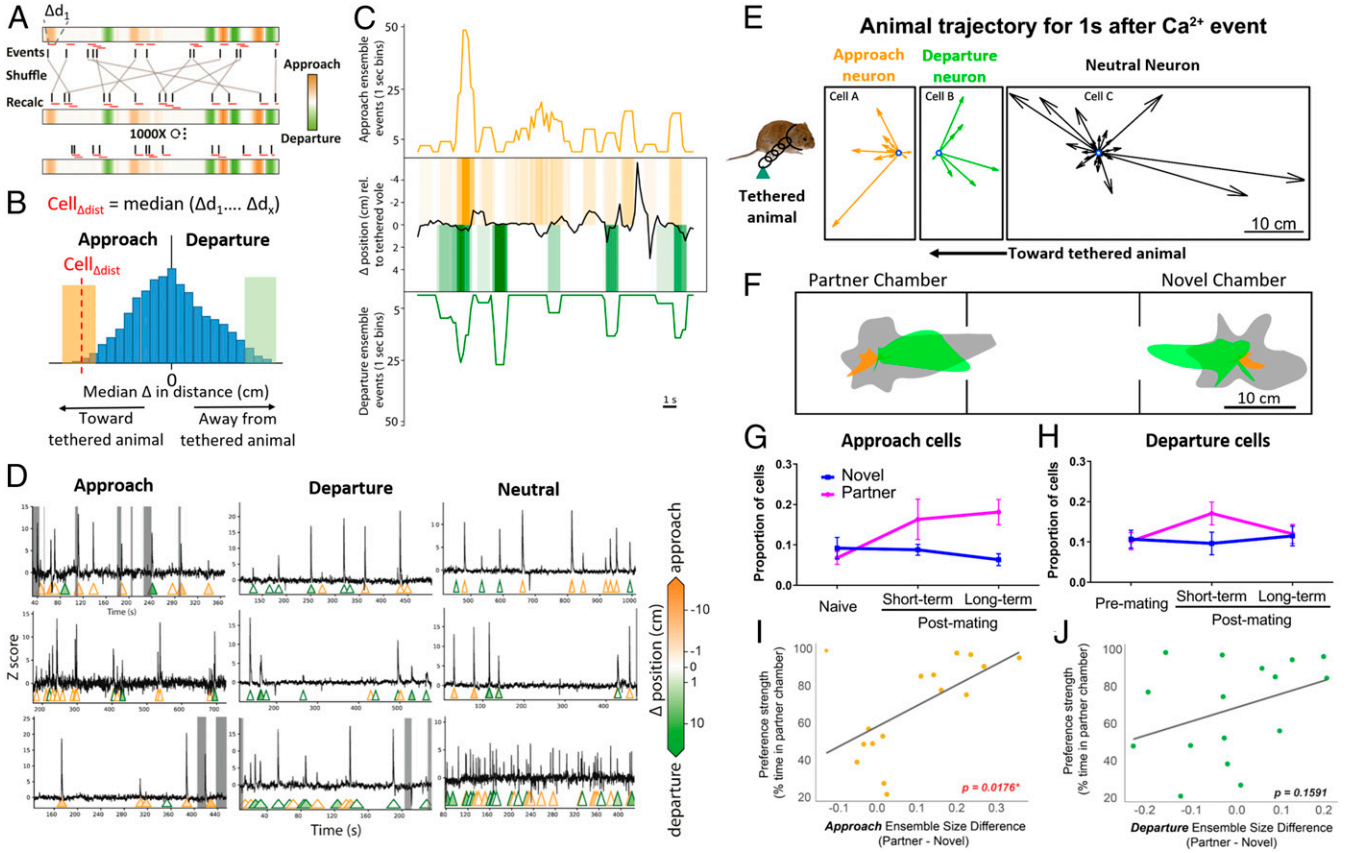

Fig. 3. Approach-cell ensemble increases upon bond maturation. (*A*) We calculated the change in distance (Δd) between the test animal and the tethered animal in the 1 s following each Ca^{2+} event (thin red rectangles) for a given cell when the animal was in the partner chamber or in the novel chamber, respectively. Event times were randomly shuffled 1,000 times, while leaving behavior data intact, to generate a null probability model. (*B*) The median distance change was compared to a null probability distribution. Cells with an observed distance change ≥95% of the null distribution (green region) were defined as departure cells and those ≤5% as approach cells (orange region). (*C*) Aggregate approach (orange) and departure (green) ensemble activity relative to test animal's movement (black line). When the black line is <0, it indicates approach; when it is >0, it indicates departure. (*D*) Example approach, departure, and neutral cells. Each Ca^{2+} event is indicated by a triangle. Green and orange denote approach/departure with intensity signifying speed. The internal color of the triangle indicates the magnitude of approach or departure. Regions in gray are where the animal briefly left the chamber containing the tethered animal. (*E*) Examples of approach, departure, and neutral neurons. Individual vectors represent change in distance from the stimulus animal during the 1 s following a Ca^{2+} transient and are plotted from the same origin. (*F*) Aggregate vector maps for approach (orange), departure (green), and neutral (gray) cells with all transients normalized to the center of the partner or novel chamber. (*G*) The proportion of partner and novel-approach neurons does not differ at the naive time point, but significantly more partner-approach neurons were identified at the long-term imaging session ($P = 0.021$). (*H*) The proportion of partner and novel departure cells did not differ at any time point. All error bars are SE. (*I*) Differences in approach ensemble size (partner – novel) are correlated with partner preference strength at the long-term time point when bonds have matured ($\rho = 0.589$, $P = 0.018$). (*J*) In contrast, differences in departure ensemble size are not correlated with partner preference ($\rho = 0.369$, $P = 0.159$). The relationship between ensemble size and partner preference for each animal at other time points is shown in *SI Appendix*, Fig. S6. Data are available at https://doi.org/10.6084/m9.figshare.8330150.

with their mate compared to with a novel conspecific—engaging in shorter social bouts during novel interactions (Fig. 2*A*)—we needed to disentangle the effect of these differences in our analysis. We chose to use a mixed-effects model as these models are ideal for fitting multiple covariates and are more robust to structured data as compared to standard linear models. Using this approach, our main question was whether the overall population Ca^{2+} event rate varied as a function of tethered vole (partner/novel) and by imaging session. We accounted for differences in bout duration, number of bouts, imaging session, tethered vole (partner/novel), and sex as fixed effects, with individual vole as a random effect, to identify factors that are significant predictors of neuronal activity (*SI Appendix*, Fig. S3). We found robust activation of the NAc during social interaction; however, after accounting for differences in the total number of social bouts and social bout duration, there were no differences in average neuronal activity between partner and novel interactions.

Specifically, we tested three hypotheses. First, based on our behavioral data, we anticipated that the largest differences in activity would be observed at the long-term time point when partner preference was most robust. We found that there was no statistically significant difference in activity when the test vole was interacting with partner and novel voles at the long-term time point ($P = 0.590$, $\chi^2 = 0.291$, df = 1). Ignoring sex, we still found no significant difference in calcium event rates between partner and novel voles at this time point ($P = 0.520$, $\chi^2 = 0.413$, df = 1). Second, we then compared rates across all three imaging sessions, combining partner interaction from the short-term and long-term imaging sessions ("partner") and combining all interactions at the naive time point with novel interaction during the short-term and long-term time points ("novel"). There was no statistically significant difference ($P = 0.281$, $\chi^2 = 1.162$, df = 1) in event rates when interacting with partner or novel voles. Again when ignoring sex, we found no significant difference ($P = 0.269$, $\chi^2 = 1.224$, df = 1). Finally, we asked whether type of interacting vole and imaging session matter, comparing six groups: partner-naive, novel-naive, partner-short term, novel-short term, partner-long term, and novel-long term. This mixed-effects model showed that there was no statistically significant difference in rates across partner and novel interaction and imaging session ($P = 0.062$, $\chi^2 = 10.498$, df = 5). Ignoring sex, we still found no significant difference in rates across the six groups ($P = 0.061$, $\chi^2 = 10.535$, df = 5). While the natural log of social bout duration, the natural log of the bout number, and a random effect for the individual vole itself were statistically significant predictors of event rates, the partner versus novel identity of the tethered vole was not statistically significant (*SI Appendix*, Fig. S3*C*). Thus, overall population event rates are not a reliable indicator for distinguishing partner versus novel vole or the imaging session (naive, short term, or long term) (13). Our findings indicate that encoding of pair bonds in the NAc does not occur via population-wide changes in activity.

Approach-Cell Ensemble Expansion Mirrors Emergence of Partner Preference. We next asked whether activity in specific subpopulations of neurons might encode features of a pair bond. We used a Ca^{2+} event-triggered analysis to identify putative neurons in which the transients corresponded with a subsequent approach to or departure from the partner or novel animal, separately. For each cell, we calculated the median change in distance between the test animal and the tethered animal during a 1-s bin immediately following each Ca^{2+} event (Fig. 3*A*). We compared the observed distance change to a null model derived from repeated randomization of Ca^{2+} event times in the partner chamber and in the novel chamber, respectively (Fig. 3*A*). By permuting (or "shuffling") the Ca^{2+} events of a given cell relative to the animal's behavior, we disrupted any statistical relationship that existed between events and behavior, enabling us to quantify the kinds of patterns expected purely by chance. We generated a null distribution by calculating the median distance change after each random shuffling of events, repeated 1,000 times. Cells with distance changes ≥95% of the null distribution were assigned as departure cells, and cells with distance changes ≤5%, were assigned as approach cells (Fig. 3*B*). Therefore, each cell was assigned to a partner-associated category and to a novel-associated category of approach, departure, or neutral (Fig. 3 *C*–*F* and *SI Appendix*, Fig. S4).

We reasoned that only cells with an event in the given chamber could be approach or departure cells. Thus, we calculated the proportion of cells for each vole that met criteria for approach or departure using the number of cells with at least one event in the chamber of interest as a denominator. Using this conservative method for estimating approach and departure cells, we observed an expansion in the number (proportion) of partner approach cells across imaging sessions (Fig. 3*G*) (14). There were no differences in partner and novel approach cells at the naive time point, with differences emerging post mating and becoming significant by the long-term time point, corresponding with bond maturation. Animals were included only if they had $n \geq 10$ cells with an event in the partner chamber and $n \geq 10$ in the novel chamber. Twelve voles met criteria of having at least 10 cells with events in each chamber at each imaging time point (n = 416 to 504 cells). An ANOVA with repeated measures for imaging session and interaction partner revealed a significant main effect of interacting vole on the proportion of approach cells (sphericity assumed: $F_{1, 11} = 7.252$, $P = 0.021$, $\eta^2 = 0.397$), but no main effect of imaging session ($F_{2, 22} = 2.989$, $P = 0.071$, $\eta^2 = 0.214$) and no interaction (sphericity not met—Greenhouse–Geisser: $F_{1.34, 14.7} = 0.016$, $P = 0.419$, $\eta^2 = 0.068$). We then used a post hoc paired t test to compare the proportion of partner and novel approach cells during each imaging session. Using the same cutoff for the number of required cells per animal, we identified significantly more partner approach than novel approach cells during the long-term imaging session (naive: $t_{15} = -0.771$, $P = 0.453$, d = –0.193; short term: $t_{14} = 1.387$, $P = 0.187$, d = 0.358; long term: $t_{14} = 3.626$, $P = 0.003$, d = 0.936). This finding was robust to different thresholds for attributing cell identity (approach or departure), although the total number of cells that met criteria increased as the P value thresholds were relaxed (*SI Appendix*, Fig. S5).

We also examined whether the difference in partner and novel ensemble size for approach and departure cells correlated with partner preference strength. At the long-term time point, when partner preference was observed consistently, we found a significant positive correlation between the difference in size of the partner and novel approach ensembles and strength of partner preference (Fig. 3*I* and *SI Appendix*, Fig. S6, P values in figure). The expansion of the partner-approach-cell ensemble indicates that bond maturation may result in changes in how partner approach and novel approach are represented in the NAc.

In contrast, we observed no differences in partner and novel departure cell ensemble size at any time point even though these cells were identified in the same permutation analysis (Fig. 3*H*) (main effect of tethered vole: $F_{1,11} = 1.106$, $P = 0.316$, $\eta^2 = 0.091$; main effect of imaging session: $F_{2,22} = 1.178$, $P = 0.327$, $\eta^2 = 0.097$; session × tethered vole: $F_{2,22} = 1.91$, $P = 0.172$, $\eta^2 = 0.148$). Likewise, differences in partner and novel departure ensemble size were not significantly correlated with partner preference strength (Fig. 3*J* and *SI Appendix*, Fig. S6, P values in figure). Thus, the observed differences in approach ensembles are unlikely due to an unanticipated variable because such a variable would equally affect identification of approach and departure cells.

As a control, we also asked 1) whether approach and departure cells were sensitive to the direction of travel and 2) whether the distance from the tethered animal was an important feature of approach-cell activity. To test whether approach or departure cell categories were reflective of direction of travel, we employed two additional tests. First, partner approach and novel

departure represent the same direction of travel relative to the apparatus. The same is true for novel approach and partner departure. If the direction of travel was the primary driver of activity within these cells, we would expect overlap between partner approach::novel departure and novel approach::partner departure ensembles. This was not the case. When we shuffled cell identities, we found that the overlap observed between partner approach::novel departure and novel approach::partner departure ensembles was not greater than chance ($P > 0.05$; *SI Appendix*, Table S3). In addition, we identified cells that qualified as partner approach cells when the test vole was in the same chamber as the tethered animal and when it was in the farthest chamber from the tethered vole (*SI Appendix*, Table S4). We found that cells that qualified as approach cells when the test animal was in the distant chamber were not the same as the partner approach cells that we identified when the test animal was in the same chamber as the tethered animal. This reinforces the finding that direction of travel is not a primary driver of approach-cell identity. This also suggests that proximity to the tethered animal is an important factor for approach-cell identity. Finally, we mapped approach trajectories from a handful of neurons (*SI Appendix*, Fig. S4). The tethered animal has a reasonable range of motion, making it possible for the test animal to approach from a variety of directions, and we found that transients in approach cells correspond with a range of approach trajectories relative to the apparatus, further suggesting that approach relative to the tethered animal is the most salient feature of approach-cell activity.

We also asked whether approach and departure cells differed by speed of travel. Approach and departure were initially calculated relative to the tethered animal, and we subsequently calculated the physical distance change following approach and departure cell events in the relevant chambers. There was no significant difference in the physical distance traveled following approach or departure cell events (*SI Appendix*, Table S2). The difference between relative and physical distance change, especially for approach cells, is likely explained by the tethered animal moving away from the approaching test animal. Thus, we concluded that there are no velocity-associated differences between approach and departure cells.

Approach/Departure Cell Activity Primarily Occurs Prior to Approach/Departure. We found that the majority of approach and departure cells exhibited events prior to rather than during social approach or departure, indicating that these cells may modulate the decision to approach or leave the tethered animal. The method that we used to identify approach and departure cells did not distinguish between cells for which the events preceded transition to approach or departure versus those for which events occurred during ongoing approach/departure. To determine whether approach-cell events occur primarily during or prior to approach, we carried out the same permutation analysis but calculated the change in distance between test and stimulus animal for the 1 s prior to a Ca^{2+} event to identify cells in which events consistently occurred after the test animal had already initiated approach. We found that, on average, 38.8% (range: 25 to 47.4%) of approach cells and 26.3% (range: 17.4 to 30.7%) of departure cells represented cells in which the Ca^{2+} events occurred while the animal was already approaching or departing (*SI Appendix*, Table S3). For the remaining cells, approach began after the transient, suggesting a potential behavioral transition. The relative proportion of approach or departure cells that fell into these two categories generally did not differ between partner-associated and novel-associated ensembles ($P > 0.05$; *SI Appendix*, Table S5).

Approach Ensembles Are Distinct while Departure Ensembles Overlap. Are partner and novel approach cells distinct populations? We performed a permutation analysis in which we shuffled cell identities to calculate the distribution of potential overlap among different functionally defined populations. By comparing to this null distribution, we found that partner and novel-approach neurons did not overlap more than would be expected by chance (Fig. 4*A* and *SI Appendix*, Fig. S7) (naive, $P = 0.23$; short term, $P = 0.79$; long term, $P = 0.25$), suggesting that partner and novel approach cells are independently represented in separate ensembles even prior to mating/bonding. Somewhat surprisingly, partner and novel departure cells overlapped more than would be expected by chance (Fig. 4*B* and *SI Appendix*, Fig. S7) (naive, $P = 0.004$; short term, $P = 0.014$; long term, $P = 0.019$). This overlap in departure ensembles, representing opposite directions of travel, suggests that trajectory relative to the overall apparatus is not a primary defining feature of departure cells.

Approach and Departure Ensembles Lack Topographical Organization. The anatomical organization of a cellular ensemble can provide insight into both important encoding properties of that network and the inputs shaping that network's activity (15). Both clustered and distributed cellular organization have been observed for networks involved in processing higher order cognitive variables. For example, grid cells display functional microorganization and clustering within the medial entorhinal cortex (16, 17). However, in mouse brain areas projecting into the NAc, including the medial prefrontal cortex, amygdala, and hypothalamus (6), ensembles encoding social information seem to lack meaningful spatial organization (18–20). In NAc, previous functional work suggests that there may be some spatial organization of dynorphin+ neurons involved in modulating appetitive and aversive responses (21). Thus, we asked whether approach and departure ensembles displayed spatial organization within the NAc.

We calculated the distance between each possible cell pair of the same identity within each animal at the long-term time point (i.e., when ensembles are most robust) and compared these values to the distances between all cells that did not meet identity classification criteria (nonclassified/neutral cells) (Fig. 4*C*). Novel approach, novel departure, and partner departure cell pairs were all found to have distance distributions that did not differ significantly from that of nonclassified cells (Kolmogorov–Smirnov test, $P > 0.05$). Partner approach cell pair distances did differ significantly, but these pairs tended to be farther apart rather than closer together ($P < 0.001$), suggesting a highly distributed organization. To further confirm that smaller-scale organizational patterns, such as spatially segregated clusters, did not exist in NAc, we also calculated the distance between the closest cell pair of the same identity for a given imaging field of view. We performed a similar permutation analysis as before in which we randomly shuffled the identities of every cell from a given animal at the long-term time point and recalculated the distance between nearest-neighbor cells of the same identity (Fig. 4*D*). A null distribution was created for each within-identity comparison by compiling the results of 1,000 shuffles. Only 6.81% (3/44) of nearest neighbor pairs across all animals were found to be closer than chance ($\leq 5\%$ of those in the null distribution); indeed, a higher proportion of pairs (20.54%; 9/44) was instead found to be farther apart than chance ($\geq 95\%$ of those in the null distribution). Together, these results imply that novel and partner ensembles in the NAc do not display clustering and instead exist in a spatially distributed pattern.

Discussion

The approach-to-partner neuronal ensemble expands upon bond formation and maturation, representing a neuronal substrate that may be important for maintaining pair bonds. Surprisingly, we found that partner-associated differences in overall NAc activity are not evident in pair-bonded prairie voles. Instead,

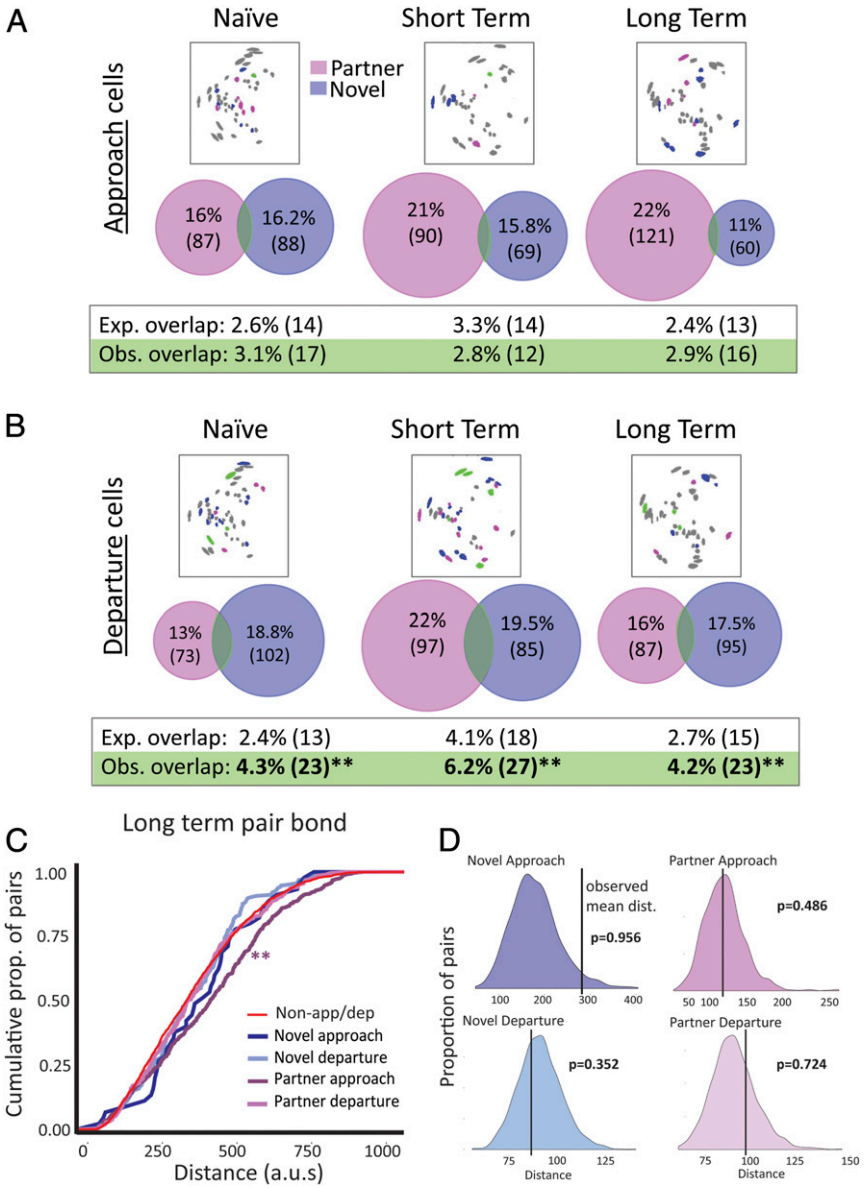

Fig. 4. Approach and departure ensemble characteristics. (*A*) The proportion of cells that belong to both partner and novel-approach ensembles is not greater than what would be expected by chance across all time points. (*B*) In contrast, departure ensembles overlap more than would be expected by chance at all three time points (**$P < 0.02$). Null distributions are shown in *SI Appendix*, Fig. S7. (*C*) Cells of the same identity are not closer together than other cells at the long-term time point. Cumulative distribution displays the proportion of within-identity cell pairs across all animals separated by a given maximal distance (*x* axis), compared to control pairs of cells that did not meet any classification criteria (red line) (**$P < 0.001$). (*D*) Null distributions of nearest neighbor pairs with the same cell identity. Horizontal line shows observed nearest neighbor distance. Example data are from one animal showing that cells comprising approach and departure ensembles are not clustered more than would be expected by chance.

specific features of pair bonds, such as the preferential desire to approach a partner rather than a stranger, may be encoded in specific neuronal ensembles. Specifically, we identified a population of neurons, the partner-approach ensemble, the activity of which corresponded with subsequent partner approach. We posit that the expansion of partner-approach ensembles following pair-bond formation may represent a mechanism for encoding key aspects of a pair bond, such as the decision to reunite with an absent pair-bonded partner.

Partner-approach neurons exhibit several features that make them ideal candidates for encoding pair-bond–related information. First, the expansion of the partner-approach ensemble closely parallels the emergence of partner preference, and differences in partner and novel ensemble size correlate with individual differences in preference strength. Second, most of these cells have Ca^{2+} transient events prior to, rather than during, ongoing approach. This would be consistent with a role for these neurons in mediating the decision to approach a particular animal. Third, the partner- and novel-approach ensembles are nonoverlapping, which would be expected if these cells contain information about the specific animal being approached. Notably, approach ensembles are nonoverlapping even at the naive time point when neither tethered animal had a significantly different familiarity or valence (both were novel opposite-sex voles), suggesting that other social cues from individual voles may be sufficient to recruit distinct approach ensembles. Finally, these ensembles are spatially distributed, an anatomical pattern similar to that found previously in upstream social ensembles in mice (18). This

patterning is consistent with ensemble coding rather than individual cell tuning or population rate coding as a unit of computation. Together, these results suggest that plasticity in the partner-approach ensemble contributes to the encoding of pair bonds.

Unlike approach ensembles, partner and novel departure ensembles overlapped more than would be expected by chance across all three time points. This difference in the properties of approach and departure ensembles further supports a functionally distinct role for these two populations. A possible interpretation of these findings is that approaching the wrong animal could have deleterious consequences (e.g., from aggression). Distinct approach ensembles may be important for identifying and deciding to approach a specific individual, while that level of specificity is not necessary when departing from a social interaction.

Being able to distinguish partner from nonpartner individuals is essential for expressing a partner preference, but there are a few aspects of our results that suggest that changes in the partner-approach ensemble are not solely a reflection of familiarity. Partner identity is likely encoded through responses to an individual odor profile, which would be learned and stabilize quickly. At the short-term time point, the test vole has been living/mating with its partner for 3 d; it is highly unlikely that partner identity has not been encoded. If the difference in the ensemble size is attributable entirely to differences in familiarity between partner and novel, it should be evident during the short-term imaging session. Instead, this difference does not emerge until the bond is behaviorally evident. Similarly, at the long-term time point, individual variation in partner preference is more likely a reflection of differences in bond strength rather than variation in perceived familiarity or the encoding of partner identity. The significant positive correlation between partner preference and relative ensemble size suggests that ensemble size reflects preference rather than familiarity per se. Finally, approach ensembles are distinct even when the test animal is exploring two novel opposite sex animals. If partner and novel ensembles were generally sensitive to familiarity versus novelty, we might expect to see significant overlap in approach neurons for the tethered animals during the naive imaging session. Thus, while familiarity is an important aspect of the bond, experience-dependent changes in approach ensembles are likely the result of behavioral factors over and above familiarity.

While our results suggest that changes in ensemble coding, especially ensemble size, may contribute to pair bonding, there are a number of limitations worth noting. Establishing Ca^{2+} imaging in voles represents a significant advance, but the specific behavioral role of approach neurons remains largely speculative without functional manipulations. Unfortunately, because these cell populations are defined by activity, rather than a particular molecular genetic component or spatial location, the methods for selectively manipulating their activity remain extremely limited and untested in voles. In addition, while we monitored the same cell population across multiple weeks as bonds formed and matured, limitations of using shared equipment made it impossible to ensure that we could repeatedly return to the same focal plane. As a result, we were unable to identify and track the same neurons across this experiment, limiting our ability to determine the potential stability of approach ensembles across time.

Prairie voles are uniquely suited to address the neuronal basis of pair bonding. They display robust behavioral changes upon bond formation, many of which are well characterized from a neuroendocrine standpoint (22). Developing novel approaches, such as the use of Ca^{2+} imaging, will be essential for uncovering how neuroendocrine mechanisms shape the neuronal basis of monogamy-associated behaviors. Ultimately, these technologies will enable us to address many of the questions stemming directly from the results presented in this study. For example, what information is recruiting cells into a partner-approach ensemble (e.g., motivational valence with development of a pair bond)? Is the choice to approach a tethered partner a critical aspect of approach cell ensemble activity/plasticity, or is the increase in approach cells seen even during interactions between two freely moving voles in a confined space? Is activity within the partner-approach ensemble required for expression of partner preference or partner-directed motivation or does the ensemble's activity simply reflect changes in activity of upstream populations, such as the prefrontal cortex (10), which may contribute to these behaviors?

In sum, we have identified a neuronal population that may underlie aspects of monogamy. Specifically, the expansion of partner-approach ensembles upon bond maturation and their activity patterns suggest a coding mechanism for partner preference, specifically for partner reunion. More broadly, this suggests that plasticity in NAc social ensembles may contribute to species differences in sociality and that alteration in NAc social ensembles may underlie dysfunctional social attachment. Thus, further understanding of social ensembles has the potential to reveal general mechanisms underlying natural social behavior variation and pathological social behavior.

Methods

All experiments were approved by the Institutional Animal Care and Use Committees at Columbia University and University of Colorado Boulder. We used miniendoscopes to perform in vivo Ca^{2+} imaging in the NAc of monogamous prairie voles choosing to interact with a mating partner or a novel vole before and after pair-bond formation. We examined the overall population activity (Ca^{2+} events/cell/second) during periods of social interaction and identified putative neurons the activity of which preceded approach to or departure from a tethered stimulus animal (partner or novel). We then characterized approach-to-partner neurons based on their activity and spatial organization. Detailed experimental methods are available in *SI Appendix*.

Code and Data Availability. MATLAB scripts are available from the Donaldson Lab GitHub repository at https://github.com/donaldsonlab/monogamousreunion. Additional data supporting the findings of this study are available on Figshare at https://doi.org/10.6084/m9.figshare.8330102, https://doi.org/10.6084/m9.figshare.8330111, and https://doi.org/10.6084/m9.figshare.8330150.

ACKNOWLEDGMENTS. We thank the animal care staff at Columbia University and University of Colorado Boulder; Saranna Rotgard, Katelyn Gordon, and Ashley Cunningham for providing additional technical assistance; Larry Young for providing colony founder voles; and René Hen and NYSTEM Core for providing access to an Inscopix miniscope. For verification of lens placement, we used microscopes housed in the University of Colorado Boulder Molecular, Cellular, and Development Biology Light Microscopy Core Facility. This work was supported by NIH award DP2OD026143 and funds from the Whitehall Foundation and the Dana Foundation (to Z.R.D.).

1. D. G. Kleiman, Monogamy in mammals. *Q. Rev. Biol.* **52**, 39–69 (1977).
2. D. Lukas, T. H. Clutton-Brock, The evolution of social monogamy in mammals. *Science* **341**, 526–530 (2013).
3. J. R. Williams, C. S. Carter, T. Insel, Partner preference development in female prairie voles is facilitated by mating or the central infusion of oxytocin. *Ann. N. Y. Acad. Sci.* **652**, 487–489 (1992).
4. L. L. Getz, C. S. Carter, L. Gavish, The mating system of the prairie vole Microtus ochrogaster: Field and laboratory evidence for pair bonding. *Behav. Ecol. Sociobiol.* **8**, 189–194 (1981).
5. S. Ikemoto, J. Panksepp, The role of nucleus accumbens dopamine in motivated behavior: A unifying interpretation with special reference to reward-seeking. *Brain Res. Brain Res. Rev.* **31**, 6–41 (1999).
6. H. Walum, L. J. Young, The neural mechanisms and circuitry of the pair bond. *Nat. Rev. Neurosci.* **19**, 643–654 (2018).
7. A.-K. Kreuder *et al.*, How the brain codes intimacy: The neurobiological substrates of romantic touch. *Hum. Brain Mapp.* **38**, 4525–4534 (2017).
8. S. L. Resendez *et al.*, Dopamine and opioid systems interact within the nucleus accumbens to maintain monogamous pair bonds. *eLife* **5**, e15325 (2016).

9. B. J. Aragona *et al*., Nucleus accumbens dopamine differentially mediates the formation and maintenance of monogamous pair bonds. *Nat. Neurosci.* **9**, 133–139 (2006).
10. E. A. Amadei *et al*., Dynamic corticostriatal activity biases social bonding in monogamous female prairie voles. *Nature* **546**, 297–301 (2017).
11. S. L. Resendez *et al*., Visualization of cortical, subcortical and deep brain neural circuit dynamics during naturalistic mammalian behavior with head-mounted microscopes and chronically implanted lenses. *Nat. Protoc.* **11**, 566–597 (2016).
12. Z. R. Donaldson, Figure 1 data. Figshare. https://doi.org/10.6084/m9.figshare.8330102. Deposited 26 June 2019.
13. Z. R. Donaldson, Figure 2 data. Figshare. https://doi.org/10.6084/m9.figshare.8330111. Deposited 26 June 2019.
14. Z. R. Donaldson, Figure 3 data. Figshare. https://doi.org/10.6084/m9.figshare.8330150. Deposited 26 June 2019.
15. R. Yuste, From the neuron doctrine to neural networks. *Nat. Rev. Neurosci.* **16**, 487–497 (2015).
16. Y. Gu *et al*., A map-like micro-organization of grid cells in the medial entorhinal cortex. *Cell* **175**, 736–750.e30 (2018).
17. J. G. Heys, K. V. Rangarajan, D. A. Dombeck, The functional micro-organization of grid cells revealed by cellular-resolution imaging. *Neuron* **84**, 1079–1090 (2014).
18. L. Kingsbury *et al*., Correlated neural activity and encoding of behavior across brains of socially interacting animals. *Cell* **178**, 429–446.e16 (2019).
19. Y. Li *et al*., Neuronal representation of social information in the medial amygdala of awake behaving mice. *Cell* **171**, 1176–1190.e17 (2017).
20. R. Remedios *et al*., Social behaviour shapes hypothalamic neural ensemble representations of conspecific sex. *Nature* **550**, 388–392 (2017).
21. R. Al-Hasani *et al*., Distinct subpopulations of nucleus accumbens dynorphin neurons drive aversion and reward. *Neuron* **87**, 1063–1077 (2015).
22. Z. V. Johnson, L. J. Young, Oxytocin and vasopressin neural networks: Implications for social behavioral diversity and translational neuroscience. *Neurosci. Biobehav. Rev.* **76**, 87–98 (2017).